International Journal of Engineering Research and Modern Education (IJERME)
ISSN (Online): 2455 - 4200
(www.rdmodernresearch.com) Volume I, Issue I, 2016

DESIGN AND IMPLEMENTATION OF A PSO BASED MOVING BEARING POSITION CONTROLLER FOR VIBRATION REDUCTION IN FAN – BEARING – ROTOR SYSTEM

Mauwafak A. Tawfik*, Mohammed I. Abu-Tabikh* & Adil A. Nayeeif**

* Assistant Professor, Mechanical Engineering Department, University of Technology, Baghdad, Iraq

** Assistant Lecturer, Mechanical Engineering Department, Al-Mustansiryah University, Baghdad, Iraq

Abstract:

An analytical and experimental study is carried out to investigate the effect of bearing position, through using PID controller, to reduce the vibration level of a centrifugal fan – bearing – rotor system. A learning algorithm for dynamic recurrent Elman neural networks based on an improved particle swarm optimization depended on experimental the data of the root mean square value developed. The proposed algorithm computes concurrently both the evolution of network structure, weights, initial inputs and used feed forward percepteron. A dynamic identifier is constructed to perform reduction in vibration level and a controller is designed to obtain reduction in vibration response for moving journal bearing along the alignment rotor. Numerical experiments show that the identifier PID controller and reduction in vibration based on the proposed algorithm can both achieve higher convergence precision and speed. An improvement in reducing the vibration is obtained through the control system by changing the position of the bearing in addition to the effect of PID controller. The percentage of improvement in the response before and after control is (79.7%) at maximum value and (50%) at minimum value for horizontal direction. And (95.24%) at maximum value and (80%) at minimum value for vertical direction. The measured experimental data is satisfied with the training process for structure of ANN after applying the particle swarm optimization at both directions, the error is 0.13 at (1000 iterations). The results for response testing by ANN structure exhibits very good agreement for both horizontal and vertical directions.

Key Words: Artificial Neural Network, Particle Swarm Optimization, Machine Learning, Vibration, Evolutionary Programming& Feed Forward Neural Networks

1. Introduction:

Tuning of bearing of rotor – bearing system is one of important feature in controlling the dynamic response of the designed system .The act of bearing position tuning can be applied to many rotary machines like fans and pumps to change the vibration to accepted level. All mechanical systems composed of mass, stiffness and damping elements exhibit vibratory response when subject to time-varying disturbances. The prediction and control of these disturbances is fundamental to the design and operation of mechanical equipment. In particular, the use of secondary, active inputs to the system in order to modify the system response in a controllable way is the topic of this work. The analysis of controlled systems is founded on the same analytical approaches used to study the vibrations of elastic structures. T˚uma et al [1] designed a test stand for investigation of the influence of bearing bushing movement control on behaviour of a rigid rotor supported in sliding journal bearings. The stand was equipped with two pairs of piezoactuators, enabling to move each bearing bushing in two directions, and with two pairs of relative sensors tracing shaft movement at both

bearings. Some results of the rotor behaviour with and without piezoactuator action were presented. Ortega *et al* [2] Presented an active vibration control scheme to reduce unbalance induced synchronous vibration in rotor-bearing systems supported on two ball bearings, one of which could be automatically moved to control the effective rotor length and, as an immediate consequence, the rotor stiffness. This dynamic stiffness control scheme, based on frequency analysis, speed control and acceleration scheduling, was used to avoid resonant vibration of a rotor system when it passes (run-up or coast down) through its first critical speed. Some numerical simulations and experiments were included to show the unbalance compensation properties and robustness of the proposed active vibration control scheme when the rotor was started and operated over the first critical speed. Tu˚ maa *et al* [3] developed a prototype of a system for the active vibration control of journal bearings with the use of piezoactuators. The controllable journal bearing was a part of a test rig, which consists of a rotor driven by an inductive motor. The actively controlled journal bearing consists of a movable bushing, which was actuated by two piezoactuators. The journal vibration was measured by a pair of proximity probes. As it was proved by experiments the active vibration control extends considerably the range of the operational speed. Reddya, and Sekharb. [4] Proposed a method to identify unbalance and looseness in rotor bearing system using artificial neural networks (ANN) by two different methods, one was by statistical features and the second by amplitude in frequency domain. In the first case statistical features were used to train and test the ANN, and in the second case amplitude in frequency domain was used to train and test the ANN. Various statistical features and amplitudes in frequency domain were extracted separately and were fed to neural network. It was observed that statistical features were giving good results over frequency domain amplitudes. Goran *et al* [5] Used active magnetic bearing (AMB) which suspends the rotating shaft and maintains it in levitated position by applying controlled electromagnetic forces on the rotor in radial and axial direction .Although the development various control method was rapid, PID control strategy was still the most widely used control strategy in many applications, including AMBs. In order to tuned PID controller, a particle swarm optimization (PSO) method was applied. Therefore, a comparative analysis of particle swarm optimization (PSO) algorithms was carried out, where two PSO algorithms, namely (1) PSO with linearly decreasing inertia weight (LDW – PSO), and (2) PSO algorithm with constriction factor approach (CFA – PSO), were independently tested for difference PID structures. The computer simulations were carried out with the aim minimizing the objective function defined as the integral of time multiplied by the absolute value of error.

In the present work an analytical and experimental study is carried out to investigate the effect of bearing positions, through using PID controller, to reduce the vibration level of a centrifugal fan – bearing – rotor system. Different rotational speed conditions under the effect of fluid forces acting on the fan impeller will be considered. Multi identification PID controller according to variable speed is built through using artificial neural network (ANN) and particle swarm optimization (PSO).

2. Design of Neural Network Structure:

In a supervised leaning ANN, a feed-forward multilayered perceptron neural networks is widely used and many enhancements have been explored as shown in figure (1). The partitioning method is one of the enhancements. The process of developing an artificial neural network based on load forecasting can be divided into 5 steps [6]:

- ✓ Selection of input variables.
- ✓ Design of neural network structure.
- ✓ Extraction of training, test and validation data.
- ✓ Training of the designed neural networks.
- ✓ Validation of the trained neural networks.

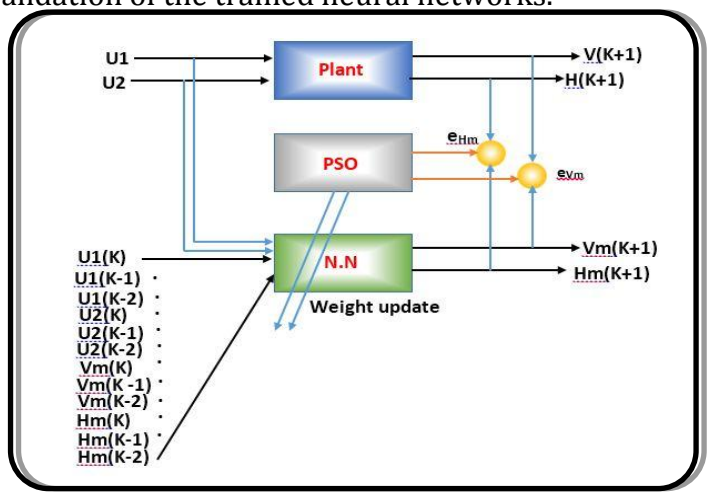

Figure 1: Structure of the Identification Method

The simplest and most common artificial neural networks use one-way signal flow. There are no delays in the feed forward artificial neural networks, the process advances to the inputs to outputs. Output values are compared with the desired output value and weights are updated with obtained error signal [7]. Feed forward network model is shown in Figure (2).

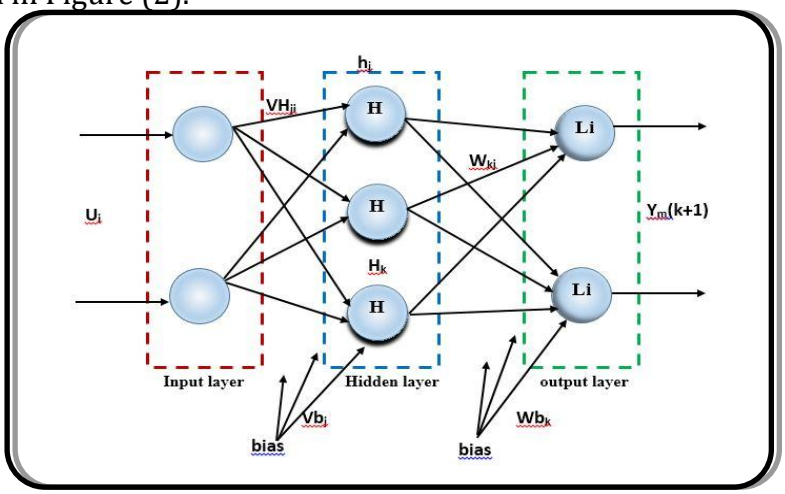

Figure 2: Modified Elman Recurrent Neural Networks

In general, system identification is to determine the model structure and parameters for a dynamic system based on the measurable input and output data of the system [8].The interest is focuses on nonlinear multi input multi output (MIMO) system identification of optimum position of moving journal bearing to reduce vibration of system using the modified Elman recurrent neural network structure to construct the position for simple of an artificial neuron.

3. Modification of PID Neural Network:

Depicts the control loop containing the neural network used for updating the controller parameters. The neural network inputs are the set point, output and error signals of the system, and the outputs generated by the neural network are the parameters of the adjusted model of the system. These parameters are used for

calculating the proportional, integral and derivative actions. Performance of this direct controller which performs an adaptive control through online learning process has been studied and compared with conventional adaptive PID controllers. Figure (3) shows the controller with a simple feed forward neural network structure, so it has three layers [9].

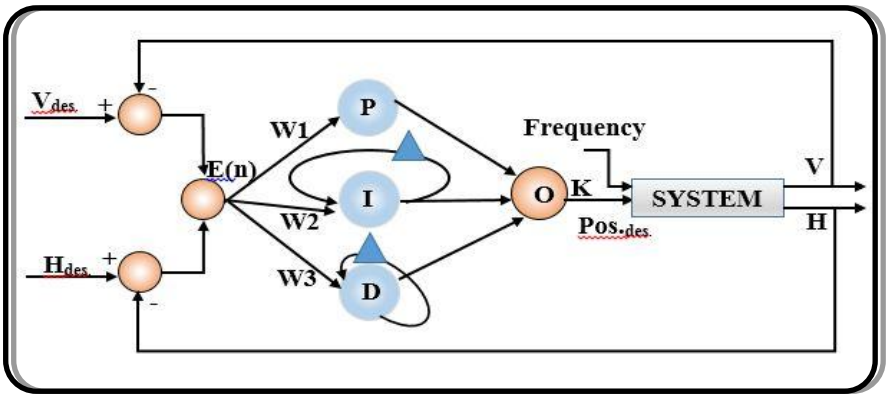

Figure 3: Structure of PIDNN

There proportional neurons in input layer with following activation function. One for receiving system setting and other for receiving process output.

$$P = O_i(k) = \begin{cases} 1 & net_i(k) > 1 \\ net_i(k) - 1 \le net_i(k) \le 1 & \ldots (1) \\ -1 & net_i(k) < -1 \end{cases}$$

In the hidden layer three neuron of different type of proportional, integral and derivative neuron exist. The activation function for integral neuron is as followed.

$$I = O_j(k) = \begin{cases} 1 & O_j(k) > 1 \\ O_j(k-1) + net_j(k) & -1 \le O_j(k) \le 1 \\ -1 & -1 < O_j(k) \end{cases} \quad \ldots (2)$$

And the activation function for derivative neuron is as followed.

$$D = O_j(k) = \begin{cases} 1 & O_j(k) > 1 \\ net_j(k) - net_j(k-1) & -1 \le O_j(k) \le -1 \\ -1 & -1 < O_j(k) \end{cases} \quad \ldots (3)$$

In the hidden layer, the neurons inputs are

$$net_i = \sum_{i=1}^{2} w_{ij} O_j \ldots (4)$$

Where i is the number of neuron in hidden layer and j is the number of neuron in input layer. Finally hidden layer is comprised of one proportional neuron which produces controller output while its neuron input is

$$net_o = \sum_{j=1}^{3} w_{oj} O_j \ldots (5)$$

Where j is the number of neuron in hidden layer and O is the output layer's single neuron. Learning of this network is done through online back-propagation algorithm. Objective function for this algorithm is as follow and the aim of the PIDNN is to minimize this objective function.

$$J = \frac{1}{N}\sum_{k=1}^{N}\left[r(k) - y(k)\right]^2 \dots (6)$$

Where N is the total number of sampling interval

$$\text{netu} = \sum(P + I + D) \dots (7)$$

4. Particle Swarm Optimization (PSO) Technique:

Particle swarm optimization (**PSO**) is a stochastically global optimization method that belongs to the family of Swarm Intelligence and Artificial Life. The conventional evolutionary equations of particle swarm optimization are as follows:

$$v_{j+1}^{i} = w_i v_j^i + c_1 r_1 \left(p_j^i - x_j^i\right) + c_2 r_2 \left(p_j^g - x_j^i\right) \dots (8)$$

Where c_1 and c_2 are positive constants and r_1 and r_2 are uniformly distributed random numbers. It is worth mentioning that the second term represents the cognitive part of PSO where the particle changes its velocity based on its own thinking and memory. The third term represents the social part of PSO where the particle changes its velocity based on the social-psychological adaptation of knowledge. If a particle violates the velocity limits, set its velocity equal to the limit.

$$x_{j+1}^{i} = x_j^i + v_{j+1}^i \dots (9)$$

If a particle violates its position limits at any dimension, set position at the proper limit. Figure (4), shows the general flow chart of PSO. [10]

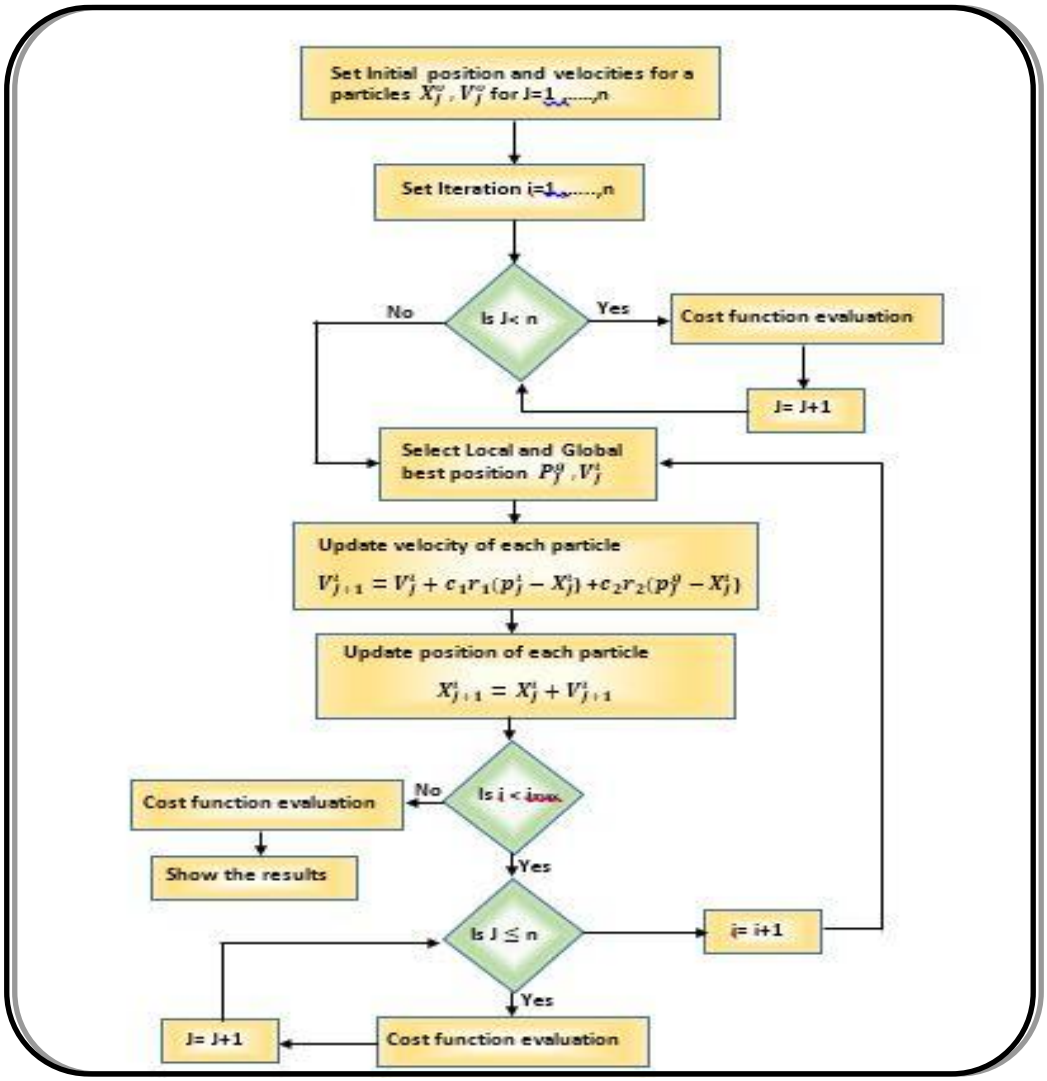

Figure 4: General Flow Chart of PSO

5. Experiment Work:

An experimental work was carried out in order to study the response of the centrifugal fan – bearing – rotor system due to moving journal bearing under the effect of fluid forces at different rotating speed condition .The model consist of many parts as shown in the figure (5).

1- Personal Computer	10- Rotor
2- AC drive	11- Ni – DAQ (6212 & 4431)
3- Support stand	12- Driver for DC motor (L298)
4- AC motor	13- DC motor
5- Centrifugal fan	14-Encoder
6- Duct	15- Sliding mechanism
7- Power supply	16- Fixed Journal bearing
8- Pitot tube with traverse	17- Moving Journal bearing
9-Coupling	

Figure 5: Experimental test rig

Centrifugal Fan Rotor:

The centrifugal fan rotor is a constant cross – section, rotor of (42 mm) diameter. Manufactured from stainless steel (416 SS). The rotor length is (480 mm), supporting by self – aligning journal bearing with span between them equal to (200 – 300 mm). The rotor is driven by a (25 hp) AC motor. To change the motor speed an AC driver is used in compatible with the motor power. The motor is connected to the main rotor by a flange – mounted universal coupling .The whole assembly, including the impeller is mounted at the other end of the rotor with an approximate mass of (14 kg), as shown in figure (6).

Journal Bearings:

Two identical. Journal bearing have been used one of them is moving the other is fixed (thrust bearing).The bearings were manufactured as three separate parts, namely

a housing (bracket) type SNG508-607 as shown in figure (7), and two brass bushes are covered by white metal, and matched interference fit into the housing, which when flush with the outer faces, provides a (5mm) circumferential groove .and (0.06 mm) clearance.

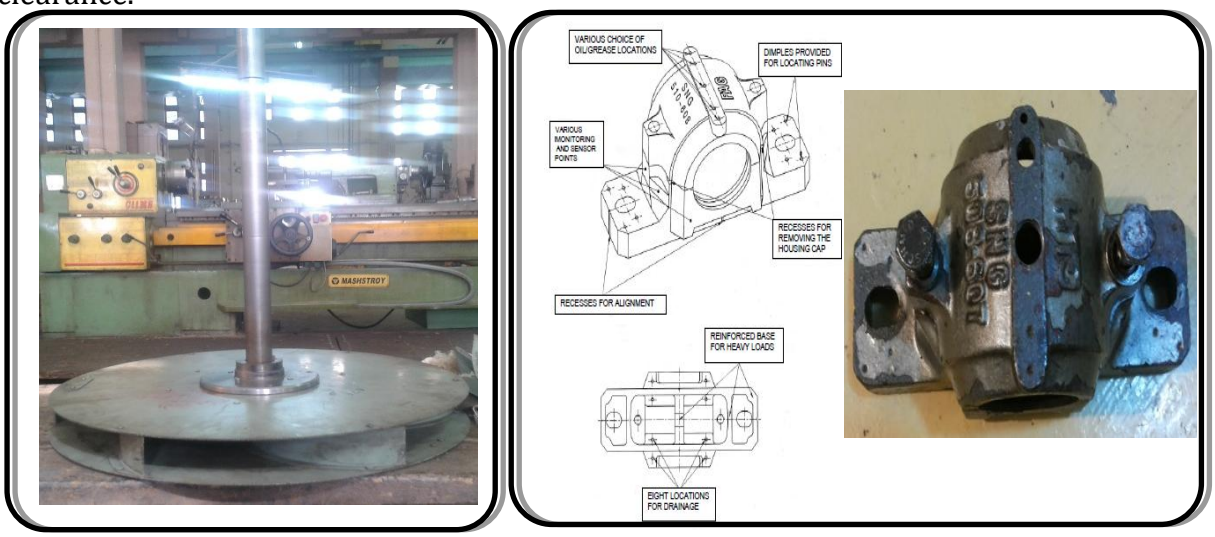

Figure 6 & 7: Housing (Bracket) Type SNG508-607

The moving bearing is fixed on a sliding block. Figure (**8**) illustrates the design of the sliding mechanism. The axial linear motion of the sliding block provided by means of screw bushing and power screw driven by D.C motor.

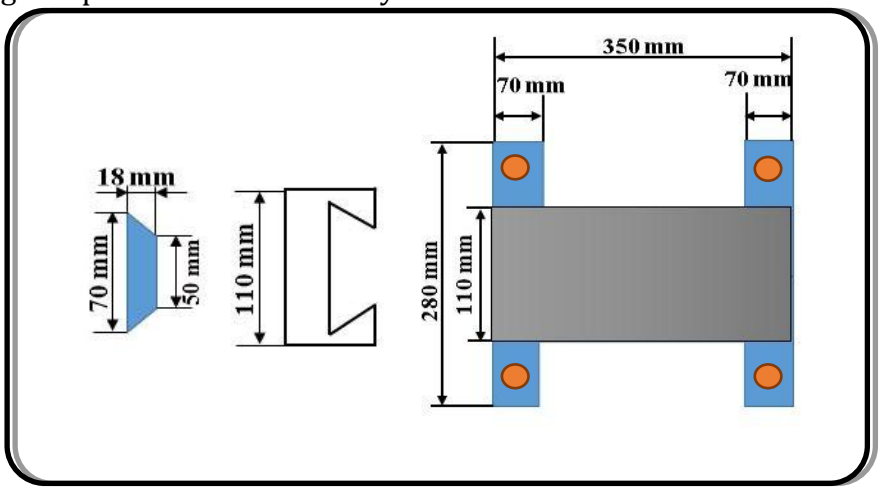

Figure 8**:** Sliding Mechanism

Vibration Measurements:

Two identical accelerometer sensors type (AC102-1A) are attached to the journal bearing housing shown in the figure (9). The sensors are fixed in two directions in order to measure the vertical and horizontal vibrations level. The signal from accelerometers are transmitted to computer by means of interface units compatible with the accelerometer type. The signal is analyzed by the LabVIEW software to determine the root mean square value (RMS), and oscillation spectrum. The specifications of sensor type shows in Table (1).

Table 1: Sensors Specifications

Sensitivity	+/-10% 100 mV/g
Frequency Response	5-15000 Hz
Dynamic Range	+50 g peak

Figure 9: Accelerometer Sensor

Data Acquisition System:

In the present work two types of data acquisition units compatible with LabVIEW software are used as shown in the figure (10).

DAQ USB-6212:

This is a multifunction (Temperature, pressure, ……, etc.). DAQ (6212) receives the measured vibration samples from DAQ (4431). The resulting outputs are manipulated by computer and send to the DC motor and encoder. The DC motor and encoder control the axial movement of the journal bearing.

DAQ USB-4431:

This unit receives vibrations signal from the accelerometer sensors which is attached to the moving journal bearing. The output signals of vibration are send to DAQ (NI-6212).Table (2) presents the technical specification of the above DAQ's.

Table 2: DAQ's Specifications

DAQ (6212)
- 32 analog inputs at 16 bits - up to 400 kS/s (250 kS/s scanning) - 2 analog outputs at 16 bits, two 32-bit - 80 MHz counter/timers
DAQ(4431)
- 24-bit analog output - 24-bit simultaneous analog inputs - ±3.5 V output range - ±10 V input range - 100 dB dynamic range - Software-selectable AC/DC , and coupling (0.1)Hz HPF

Figure 10: Data Acquisitions

In addition to DAQ units, two driver cards (L298) and (TL494) were used for the connection of DAQ (NI-6212) with the DC motor and encoder, see figures (11) and (12).

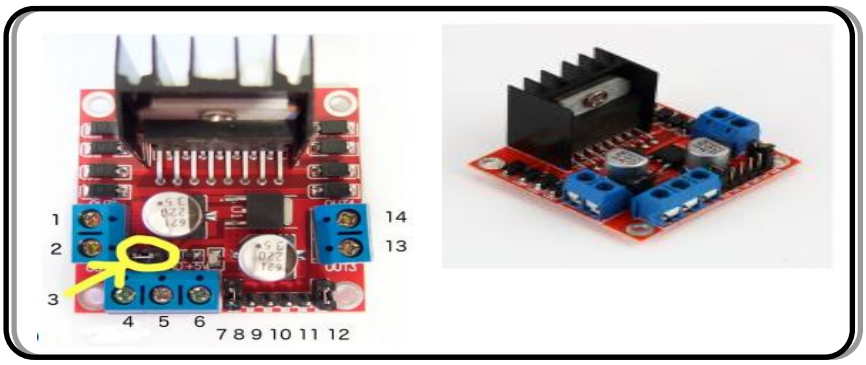

Figure 11: Driver L298

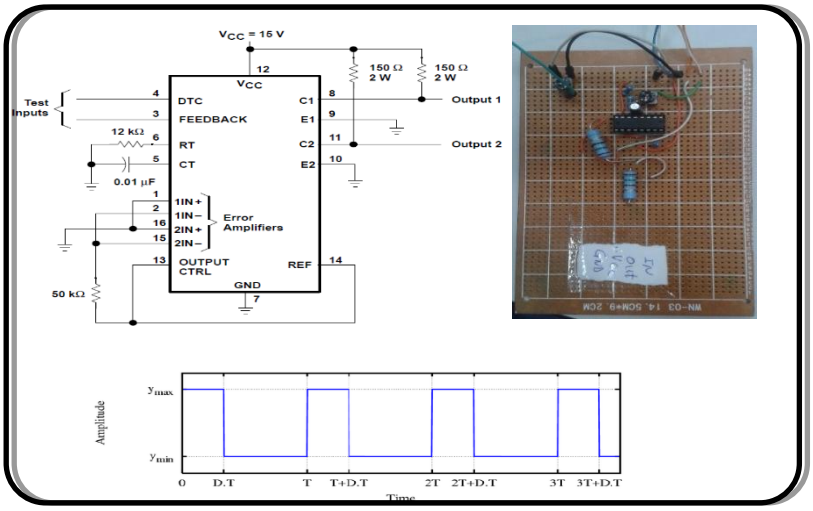

Figure 12: Test Circuit (TL494)

DC Motor with Gear and Encoder:

The moving bearing is fixed on the sliding block of the sliding mechanism. The axial linear motion of the sliding block with bearing is provided by power screw and the D.C motor. The type and specification of the D.C motor are shown in figure (13).The implemented sliding surface was designed, especially for this study; the mechanism of the sliding is composed of power screw which is coupled to a DC geared motor to transform the rotational motion from the actuator to linear motion, and then the tendons are pulled the sliding to close the distance of the span (between bearing) object.

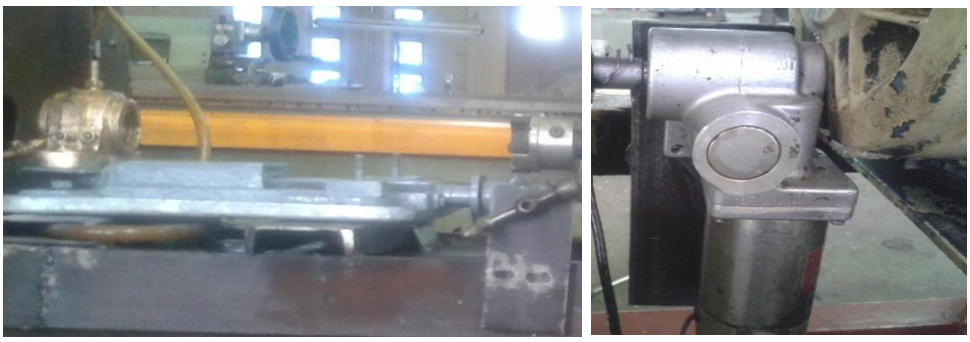

NO. (R)	**MM40**	**A-2-300**	**24V,50Hz,70 watt**
KYOEITSUSHIA company LTD		**SHIBUYA TOKYO JAPAN**	

Figure 13: DC Motor and Sliding Mechanism

A rotary encoder is used to read the number of rotation per plus. Resolution of encoder is (1024 rev/plus), and is shown in figure (14).

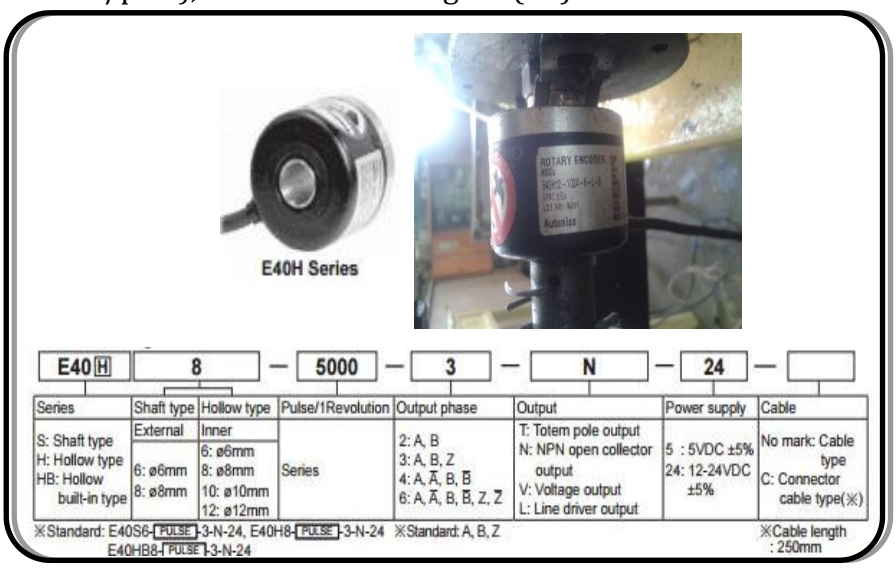

Figure 14: Rotary Encoder

Experimental Procedure:

The following experimental procedures were considered:

- ✓ Estimate experimentally the parameters of PID controller for DC motor with gear under constant speed condition
- ✓ Recording the vibration level (root mean square value) for the moving Journal bearing in vertical and horizontal directions by using accelerometers and the LabVIEW software.
- ✓ Reading the signal of vibration level (RMS) by DAQ (NI-4431) from the two sensor in vertical and horizontal directions fixed on the housing moving bearing. The signal is transmitted to the identification PID control for the system, then send to the encoder after converting the linear position to angular position. Finally the signal reaches to the board (TL494) to control the optimum position for the desire response.
- ✓ Data is Saved after (5 sec) for the wave that display on the LabVIEW program in excel file type. Changing the angular velocity by AC drive manually to increase the velocity and reading after (5 sec) until reaching the desired velocity.
- ✓ Control the system, after knowing the parameter of the PID control for the identification neural network and DC motor tuning.

6. Results and Discussion:

Figure (15) illustrates three – dimensional view of the amplitude (RMS) along the span (bearing position). It can be observed from the cited figure the peak value of vibration in general located at higher frequencies (30 – 40 Hz), also peaks at the critical speed can be obtained. Some of these peaks appears in the horizontal direction while these peaks do not appear in the vertical direction. Also it is obvious that the response of the vibration in horizontal direction is larger than that of the vertical direction, however the control system takes into account the both directions in the controlling process and choosing the optimum position for this regard.

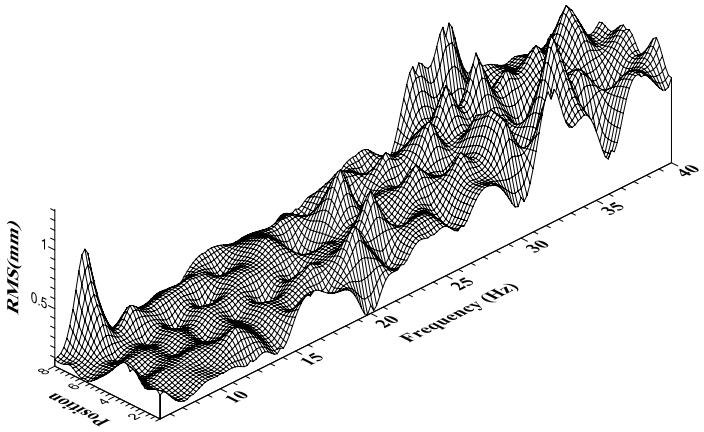

Horizontal Direction

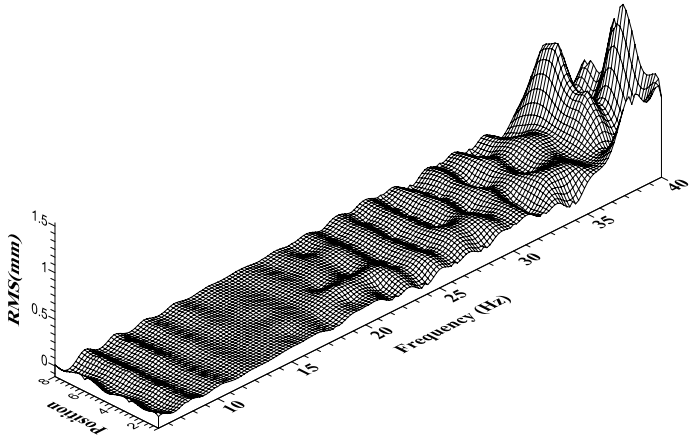

Vertical Direction

Figure 15: Amplitude Distribution along Span at Different Speeds

Figures (16) and (17) show the response of the system at each constant speed of (600 rpm, 1200 rpm, and 1800 rpm) with variable bearing positions before and after applying control concept. It can be observed from these figures when the test rig rotor runs at the designated range of speeds, the (RMS) of the amplitudes of vibration are reduced to a specific values and improvement in vibration response is obtained after applying control concept through changing the position of the bearing. It can be clearly seen from figures, as the bearing moves from position to the optimum position, all response value will be reduced in general at different speed values and at any position. This has been done firstly by locating the optimum position which gives lowest value of the RMS through the neural network. Secondly the response will be modulated through the feedback to the PID controller to have the final response values for the vertical and horizontal directions. It can be seen from figure (16) for each values of rotational speed range, the vibration response versus bearing position. This figure shows distinguish position at which the response is so high at different range of speed. For instance at position (1.2) the response is so high at different range of speed in comparison with the response at other bearing positions. Also bearing position at (2.4 and 3.4) shows the same behavior. Hence one must take into account these positions to avoid the higher response of vibration. Inspite of that the control system has the ability to control the higher response of vibration at these bearing positions. This can be clearly observe of from figure (17), at position (1.2) the response was (1.75 mm) at horizontal direction

before control and becomes (0.22 mm) after control at the same direction. Also at position (2.4 and 3.4) the response was (1.5 mm and 1.85 mm) respectively before control and they become (0.155 mm and 0.17 mm) after control for the horizontal directions. This shows higher improvement in reducing the vibration through the control system by changing the position of the bearing and in addition to the effect of PID controller. Improvement percentages for the cited bearing position are (87.4%, 89.6%, and 90.8%). Also from these figure one can deduce that as the bearing position increases (i.e as the distance between the two bearing decreases the vibration response decreases after the control process). This may be attributed to the value of equivalent stiffness of the system. As this distance increases the flexibility of the system increases and the equivalent stiffness may decrease taking into account the response.

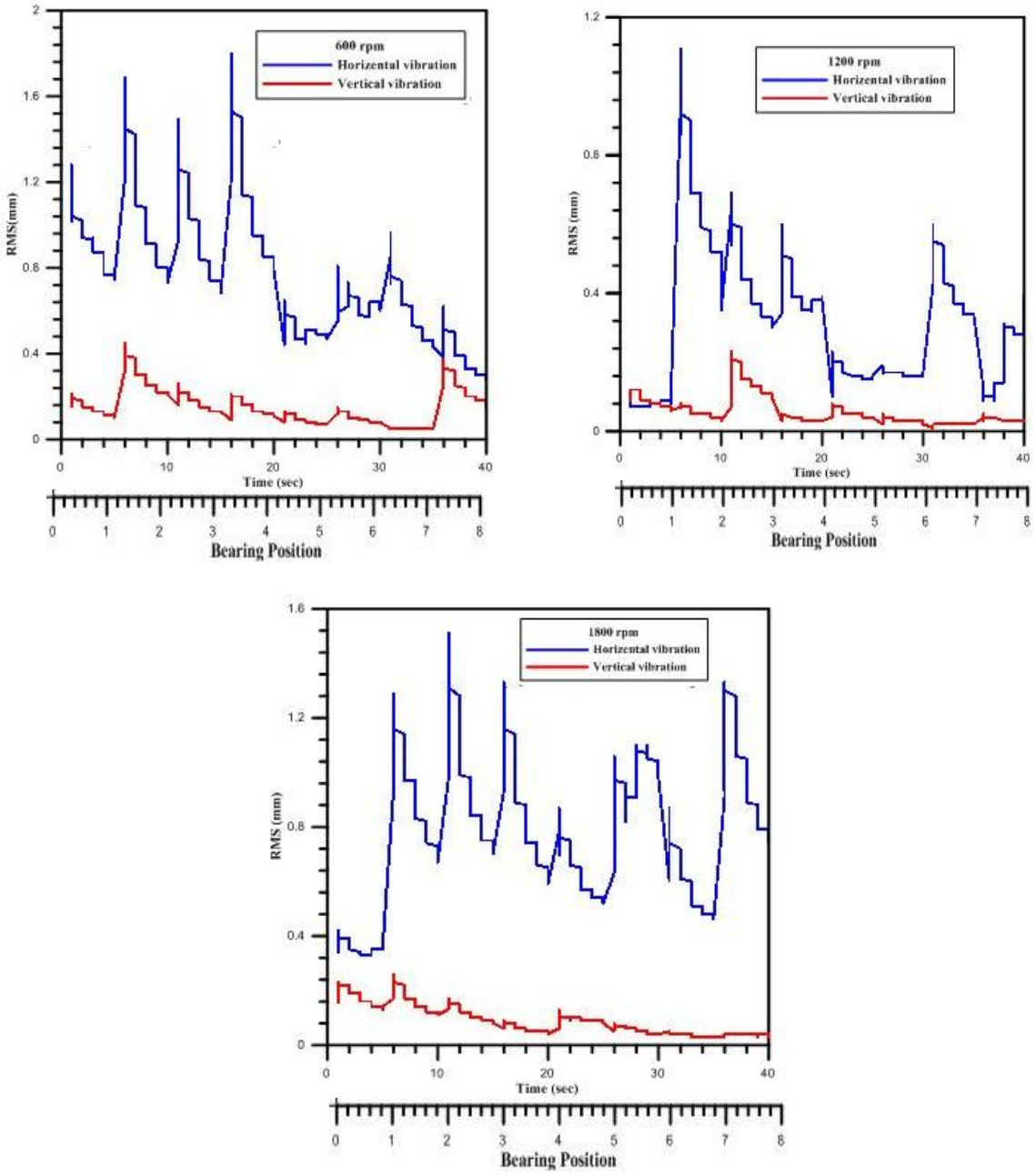

Figure 16: System Response at Different Speeds for Span Length before control

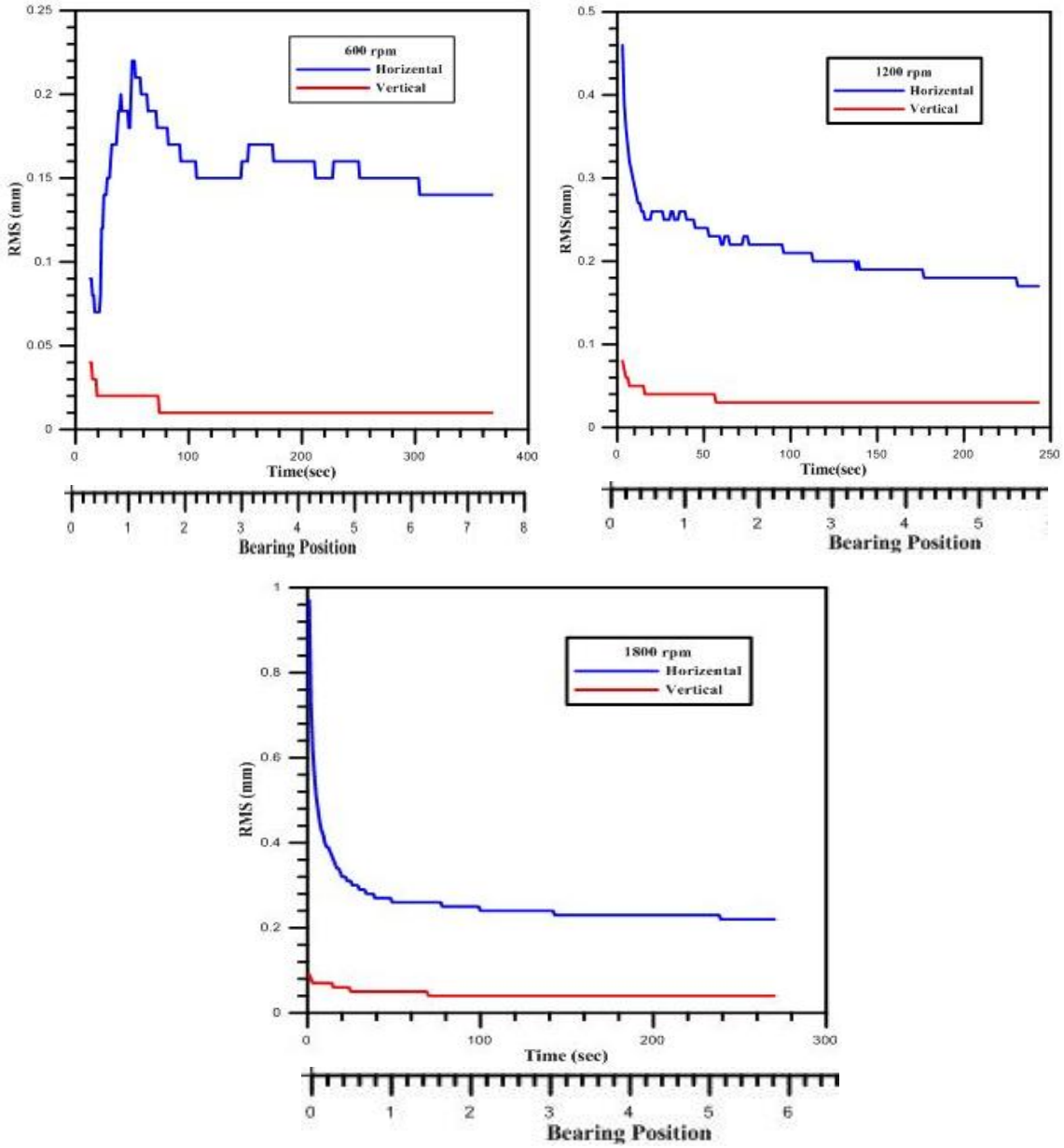

Figure 17: System Response at Different Speeds for Span Length after Control

Table (3) demonstrates the values of (RMS) for the measured values at horizontal and vertical directions before and after control, when the rig is operating at different speeds (600 rpm, 1200 rpm, and 1800 rpm) and at any bearing positions (1, 2, 3, 4, 5, 6, 7, and 8). It can be observed from the cited table at each position along the span and at rotation speed of 600 rpm, the maximum value of RMS is (0.79 mm) at position (4) and the minimum value is (0.28 mm) at position (8) for horizontal direction while at the vertical direction the maximum value is (0.21 mm) at position (2) and the minimum value is (0.05 mm) at position (7) before control. After applying control the RMS values at position (4) & (7) become (0.16 mm) and (0.14 mm) respectively for the horizontal direction, while for the vertical direction, the values of the maximum & the minimum is reduced to (0.01 mm). The percentage of improvement in the response before and after control is (79.74%) at maximum value and (50%) at minimum value for horizontal direction and (95.24 %) at maximum value and (80%) at minimum value for vertical direction. The details of improvement percentage at each speed and each position is

shown in table (4).Table (5) shows the maximum improvement as percentage along the bearing position for both directions at optimum position and rotational speed. It can be seen clearly from this table the efficient process of the control system through changing the position of the bearing in both horizontal and vertical response directions.

Table 3: Vibration level (RMS) before and after Control at each Position

Rotating speed (rpm)	Bearing position	Before control		After control	
		RMS (mm)		RMS (mm)	
		Horizontal	Vertical	Horizontal	Vertical
600	1	0.75	0.10	0.18	0.02
	2	0.73	0.21	0.16	0.01
	3	0.68	0.13	0.15	0.01
	4	0.79	0.09	0.16	0.01
	5	0.44	0.07	0.16	0.01
	6	0.55	0.08	0.15	0.01
	7	0.43	0.05	0.14	0.01
	8	0.28	0.16	0.14	0.01
1200	1	0.07	0.06	0.25	0.04
	2	0.35	0.04	0.22	0.03
	3	0.30	0.07	0.20	0.03
	4	0.34	0.04	0.19	0.03
	5	0.2	0.04	0.17	0.03
	6	0.16	0.02	———	———
	7	0.34	0.01	———	———
	8	0.09	0.03	———	———
1800	1	0.33	0.13	0.27	0.05
	2	0.67	0.11	0.25	0.04
	3	0.70	0.08	0.24	0.04
	4	0.59	0.05	0.23	0.04
	5	0.52	0.06	0.25	0.04
	6	0.63	0.05	0.22	0.04
	7	0.46	0.04	0.22	0.04
	8	0.75	0.03	———	———

Table 4: Improvement of percentage at each Position

Rotating speed (rpm)	Bearing position	Percentage of Improvement (%)	
		RMS (mm)	
		Horizontal	Vertical
600	1	76	80
	2	78.08	95.24
	3	77.94	92.3
	4	79.74	80

	5	63.63	85.71
	6	72.7	87.5
	7	67.4	80
	8	50	93.75
1200	1	-72	33.3
	2	37.14	25
	3	33.34	57.14
	4	44.12	25
	5	5	25
1800	1	18.18	61.54
	2	62.68	63.63
	3	65.71	50
	4	61.01	2
	5	51.9	33.34
	6	65.08	2
	7	52.17	0

Table 5: Improvement percentage at optimum position at different speeds

Rotating speed	Optimum position	Improvement percentage %	
		Max. horizontal	Max. vertical
600 rpm	8	77.4	97.3
1200 rpm	5.983	17.4	87.5
1800 rpm	6.61	74.7	52.1

PID Control Using ANN:

Table (6) shows the parameters of PID control and the optimum bearing position. It can be observed from the table the optimum bearing position that results in reduction of vibration due to the movement of journal bearing toward the thrust bearing at different speed conditions. Figure (18) shows the training experimental data that is used to build the structure of ANN which is described the vibration behavior at any position and at different speed conditions at the horizontal and vertical directions. It can be observed from the figure the measured data is satisfied with the training process for structure of ANN after applying the particle swarm optimization at both directions. The percentage error is (13%) after running the program at (1000 iterations), the weights are recorded at this error and iteration where the estimated parameter of identification of PID control is depended on. The results presented by the cited figure indicates a good neural training.

Table 6: PID Control Parameters and Optimum Bearing Position

Rotating speed (rpm)	W1	W2	W3	K	position
600	-1.7244	-6.0052	0.3138	11.3647	8
1200	-11.3551	1.1623	0.3833	11.5154	5.983
1800	-11.0475	1.0601	0.3385	12.0554	6.61
2400	-4.8204	-5.3609	-0.9659	13.1669	8

Figures (19) to (22) Show the results of PID control for horizontal and vertical directions at different rotation speed condition and optimum bearing position. It can be observed from these figures the optimum position is obtained when the journal bearing moving toward the thrust bearing, which in turn used to obtain the parameter of the PID control. This parameter is used in LABVIEW program after connecting online with the rig at different bearing position and speed.

Validation of Control:

Structural model of ANN has been built by using (18) inputs and only two outputs to get a possible solution. A feed forward particle swarm neural network has been adopted using MATLAB. A series of trial and error processes were performed to select the best number of hidden neurons. ANN models with different number of hidden neurons are trained and each ANN model is evaluated based on training performance. Generally the training process is satisfactory as both the training and validation performances converged at low mean square error (MSE) values. Figure (23) show the proposed neural networks for testing data to achieve the working structural model. The result for testing exhibits very good agreement for both horizontal and vertical direction.

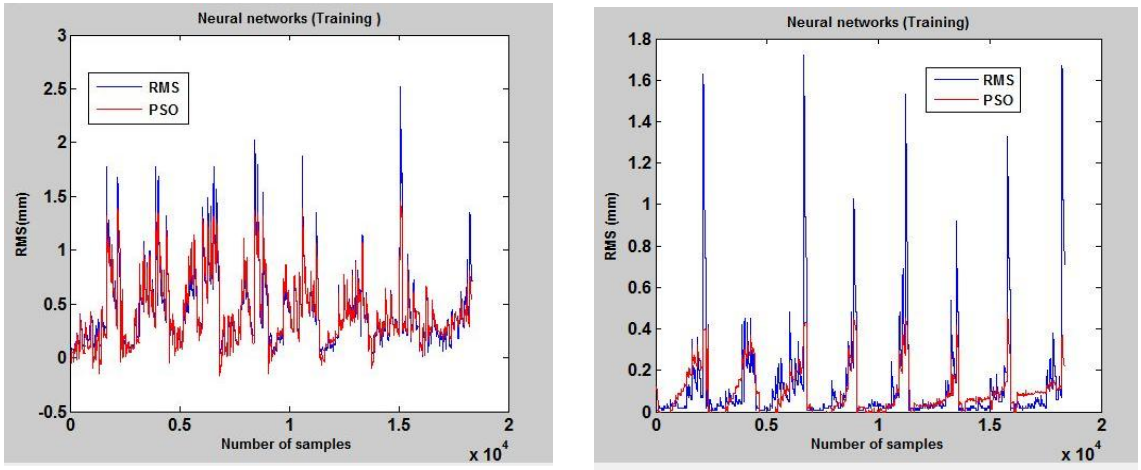

a- Horizontal direction b- Vertical direction

Figure 18: Neural Network (Training) with Particle Swarm Optimization

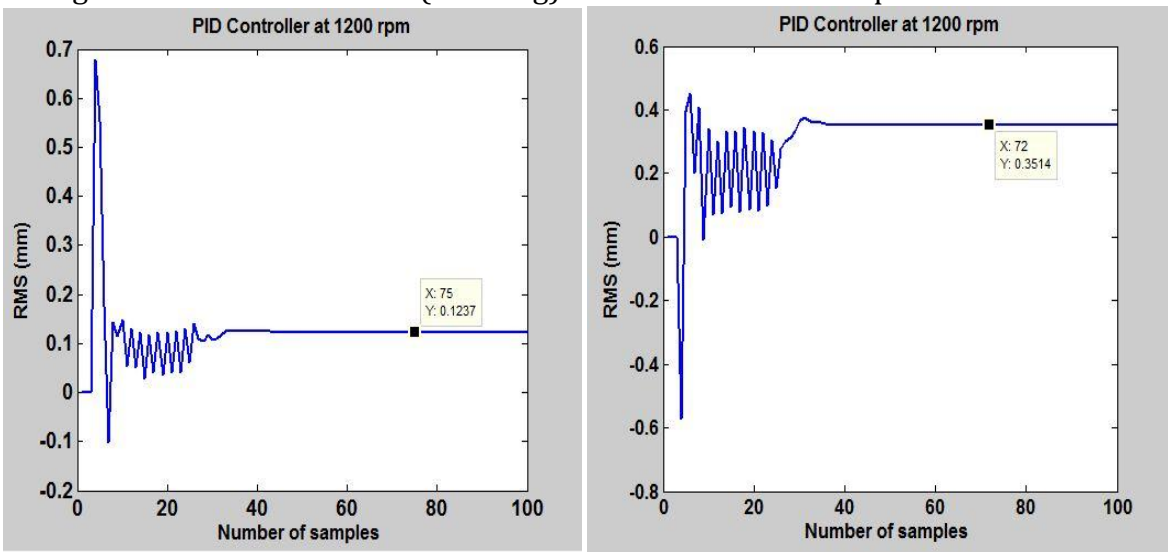

Figure 19: PID Control at 1200 rpm

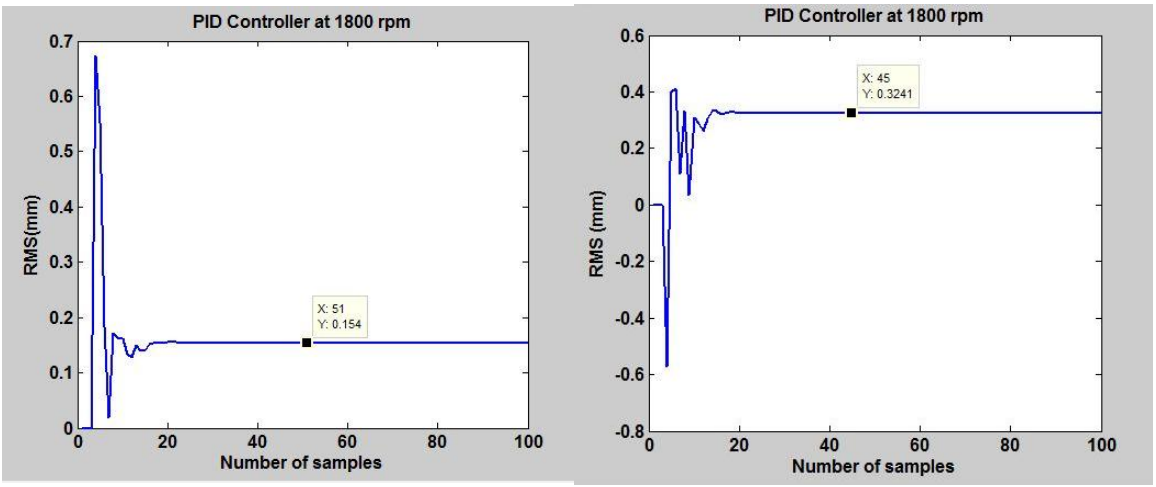

Figure 20: PID Control at 1800rpm

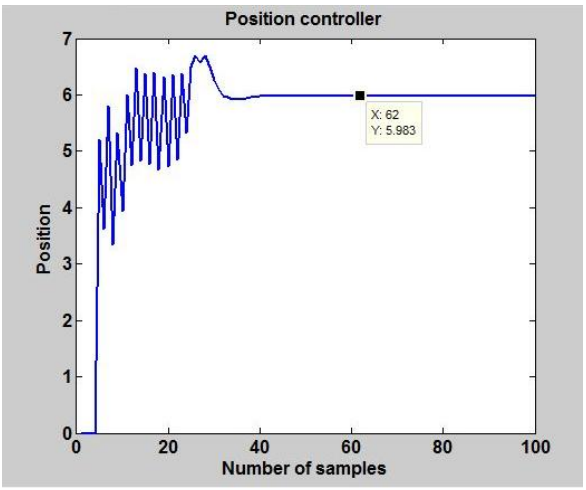

Figure 21: Positional Control at 1200rpm

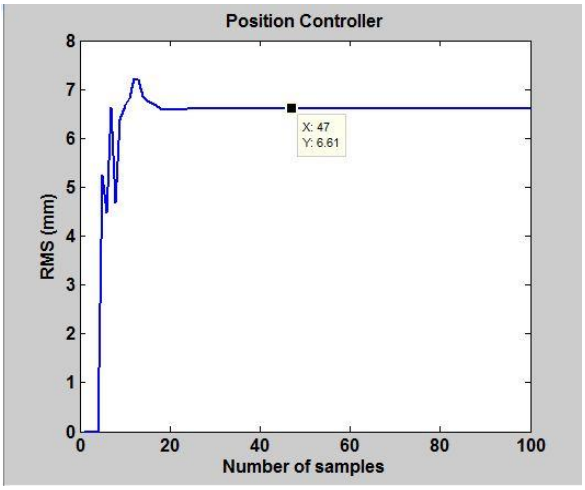

Figure 22: Positional Control at 1800rpm

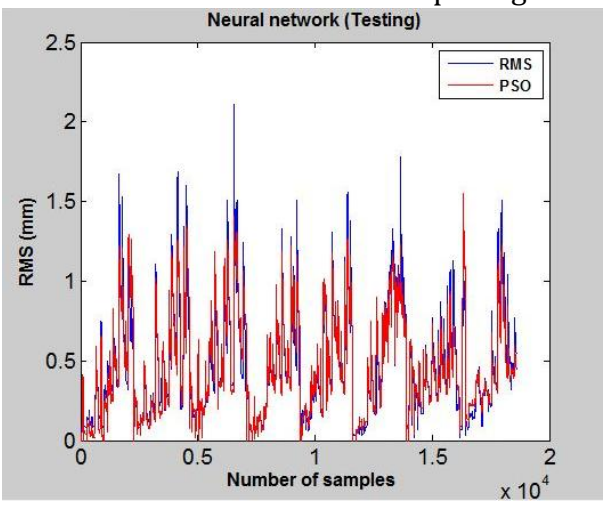

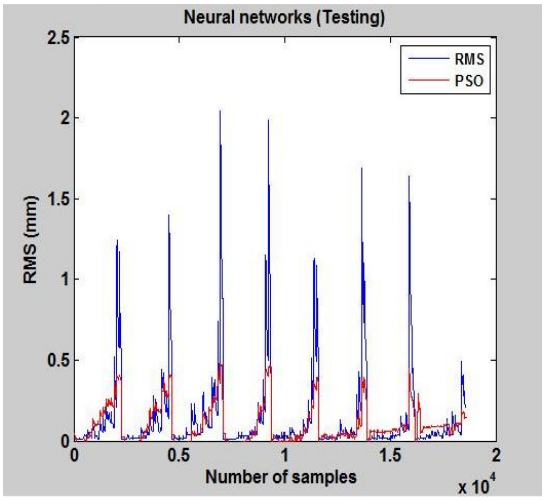

a- Horizontal direction b- Vertical direction

Figure 23: Neural Network (Testing) with Particle Swarm Optimization

7. Conclusion:

- ✓ Distinguish bearing positions are indicated at which the response is so high. These positions are taken into account to avoid the higher response of vibration.

The control system has the ability to control the higher response of vibration at these positions.

- ✓ The response of vibration in horizontal direction is larger than that of the vertical direction. The peak values of vibration at high frequencies (30 – 40 Hz) in the horizontal direction is more dominant than that in the vertical direction.
- ✓ The (RMS) of the amplitudes of vibration are reduced to specific values and the improvement in vibration response is obtained after applying control concept through changing the position of bearing.
- ✓ An improvement in reducing the vibration is obtained through the control system by changing the position of the bearing in addition to the effect of PID controller. The percentage of improvement in the response before and after control is (79.7%) at maximum value and (50%) at minimum value for horizontal direction. And (95.24%) at maximum value and (80%) at minimum value for vertical direction.
- ✓ The measured experimental data is satisfied with the training process for structure of ANN after applying the particle swarm optimization at both directions, the error is 0.13 at (1000 iterations). The result for response testing by ANN structure exhibits very good agreement for both horizontal and vertical directions.
- ✓ From the result of PID control. It is observed the optimum position is obtained when the journal bearing moving toward the thrust bearing.

8. References:

1. T˚uma , I. ; ˇSimek , J. ; ˇSkuta , J. ; Kleˇcka , R. ; ”The influence of controlled bushing movement on behavior of a rotor in sliding bearings “ , Engineering Mechanics , Vol. 17, No. 3/4, pp. (269–279) , 2010.
2. Ortega , A. B. ; Carbajal , F. B. ; Navarro , G. S. ; “ Active vibration control of a rotor-bearing system based on dynamic stiffness “ ,Article in REVISTA FACULTAD DE INGENIERÍA ·,pp.(125-133) , SEPTEMBER 2010.
3. Tu˚ maa , J. ; ˇSimek , J. ; ˇSkuta , J. ; JaroslavLos a. ; ”Active vibrations control of journal bearings with the use of piezoactuators “ , Mechanical Systems and Signal Processing ,Elsevier Ltd. All rights reserved, pp.(1 – 12), 2012.
4. Reddya, M. C. S.; Sekharb , A. S. ; ”Application of Artificial Neural Networks for Identification of Unbalance and Looseness in Rotor Bearing Systems “ , International Journal of Applied Science and Engineering , pp.(69 – 84), 2013.
5. Kanga , J. ; Menga , W. ; Abrahamc , A. ; Liuc , H. ; “ An Adaptive PID Neural Network for Complex Nonlinear System Control “ , Preprint submitted to Neuro computing , pp.(1 – 21) , February 2013.
6. Goran , S. ; Sanjin , B. ; Roberto , Z. ; ”Comparative Analysis of PSO Algorithm for PID controller Tuning “ , Chinse Journal of mechanical engineering , vol. (27) , NO. 5, 2014.
7. Zhang, G.P. “Neural networks for classification “, a survey. IEEE Transactions on Systems Man and Cybernetics, 2000.
8. springer; “ Optimization of PID Controllers Using Ant Colony and Genetic Algorithms ” , Springer Heidelberg New York Dordrecht London , 2013.
9. Shahrakia, F.; Fanaeib , M.A.; Arjomandzadeha ,A.R.; “Adaptive System Control with PID Neural Networks “ .
10. Ogata, K. “Modern control engineering “, Fourth edition, printed in the United States of America, pp. (681 – 745), 2002.

11. Tuaimah , F.M. ;Meteb ,M. F. ; ”A Particle Swarm Optimization based Optimal Power Flow Problem for Iraqi Extra High Voltage Grid “ , International Journal of Computer Applications ,Vol. 59, No.8, pp.(16-21) , December 2012
12. Tawfik ,M. A. ,Mohsin, M. I. , Nayeeif ,A. A. ,”Effect of mode of rotation and speed on the pressure field and axial thrust of Industrial centrifugal fan”,Journal of Engineering and Development , vol. (20) ,No.(2) ,2016.
13. Tandan , N. ; Swarnkar , K. K. ; “Tuning of PID Controller using Modified Particle Swarm Optimization “ , International Journal of Electronics, Electrical and Computational System IJEECS , Vol. 4, pp.(62-66), May 2015 .